



Published in final edited form as:

*J Shoulder Elbow Surg.* 2014 December ; 23(12): 1786–1791. doi:10.1016/j.jse.2014.03.002.

## The Effect of Age on Rat Rotator Cuff Muscle Architecture

Malcolm A. Swan, BS<sup>1</sup>, Eugene Sato, BS<sup>1</sup>, Leesa Galatz, MD<sup>2</sup>, Steve Thomopoulos, PhD<sup>2</sup>, and Samuel R. Ward, PT, PhD<sup>1</sup>

<sup>1</sup>Departments of Orthopaedic Surgery, Radiology, and Bioengineering, University of California and Veterans Administration Medical Centers, San Diego, CA, USA

<sup>2</sup>Department of Orthopaedic Surgery, Washington University in St Louis, St. Louis, MO, USA.

### Abstract

**Background**—Understanding rotator cuff muscle function during disease development and after repair is necessary for preventing degeneration and improving post-surgical outcomes, respectively. The rat is a commonly used rotator cuff animal model; however, unlike humans, rats continue to grow throughout their lifespan, so age-related changes in muscle structure may complicate an understanding of muscle adaptations to injury.

**Methods**—Infraspinatus and supraspinatus muscle mass, fiber length, pennation angle, sarcomere length, and physiological cross-sectional area (PCSA) were measured in Sprague-Dawley rats (n=30) ranging from 51-814 grams body mass (~3 weeks to ~18 months).

**Results**—Both the supraspinatus and infraspinatus showed a striking conservation of sarcomere length throughout growth. There was linear growth in muscle mass and PCSA, non-linear growth in muscle length and fiber bundle length, and a linear relationship between humeral head diameter and fiber bundle length, suggesting that muscle fiber length (serial sarcomere number) adjusted according to skeletal dimensions. These muscle growth trajectories allowed sarcomere length to remain nearly constant.

**Discussion**—During the typical rat rotator cuff experimental period (animal mass 400g-600g), muscle mass will increase 30%, fiber length will increase 7%, and PCSA will increase 27%, but sarcomere lengths are nearly constant. Therefore, these normal growth-induced changes in architecture must be considered when muscle atrophy or fiber shortening is measured after rotator cuff tears in this model.

### Keywords

Age; Muscle Architecture; Rotator Cuff; Shoulder; Scaling

---

© 2014 Journal of Shoulder and Elbow Surgery Board of Trustees. Published by Mosby, Inc. All rights reserved.

Address for correspondence: Samuel R. Ward, PT, Ph.D. Department of Radiology, Orthopaedic Surgery, and Bioengineering 9500 Gilman Drive (0610) La Jolla, CA 92093, USA srward@ucsd.edu.

**Publisher's Disclaimer:** This is a PDF file of an unedited manuscript that has been accepted for publication. As a service to our customers we are providing this early version of the manuscript. The manuscript will undergo copyediting, typesetting, and review of the resulting proof before it is published in its final citable form. Please note that during the production process errors may be discovered which could affect the content, and all legal disclaimers that apply to the journal pertain.

Financial Enumerations: None

## INTRODUCTION

The rotator cuff muscles and their tendinous insertions are responsible for both strength and stability in the shoulder, yet they are susceptible to age related, degenerative changes leading to tendinosis and tearing. Rotator cuff tears are common and affect approximately 30% of patients over 60 years of age.<sup>4</sup> The rotator cuff muscles undergo structural atrophy and fibrosis when torn<sup>19</sup>, altering their function, and changes do not appear to resolve after repair.<sup>6; 7</sup> Importantly, the atrophy and fibrosis associated with chronic tears has been associated with poor reparability and healing.<sup>3</sup> Therefore, an understanding of muscle function after injury and/or repair requires an understanding of muscle structure.

Muscle architecture is defined as the structural arrangement of muscle fibers relative to the axis of force generation and represents the best predictor of muscle function.<sup>2; 5; 14; 21</sup> Two common measures of muscle architecture include fiber length and physiological cross-sectional area (PCSA). Fiber length is directly proportional to excursion (the length of shortening that the muscle undergoes during a full contraction)<sup>21</sup> and velocity (the speed at which a muscle changes length).<sup>2</sup> PCSA is proportional to the maximum isometric force producing capacity of the muscle and is a direct indicator of strength.<sup>14</sup>

Since measures of muscle architecture are highly invasive and require muscle destruction, a variety of animal models have been used to study the pathology of muscles associated with rotator cuff tendon tears. The rat is a common model for assessing rotator cuff tears because of its anatomic similarities to the human shoulder<sup>15</sup> and the vast amount of physiological, behavioral, and morphological data that already exists for this species.<sup>1; 15; 19</sup> Several studies have shown that tenotomy of a healthy supraspinatus tendon in rats results in both radial and longitudinal atrophy of the supraspinatus muscle, which reduces the muscle's force generating capacity.<sup>1; 19</sup> However, the atrophic changes observed in the rat after tenotomy are significantly less severe than those observed in humans after rotator cuff tear.<sup>19</sup> In order to achieve atrophy equivalent to that observed clinically, the tenotomized muscles must also be denervated.<sup>12</sup>

One key difference between rodent models and humans is that rodent skeletons and muscles continue to grow in size over the animal's lifespan, confounding the effects of experimentally induced rotator cuff injury. For example, after measuring skeletal muscle growth over 28 days postnatal in mice, Gokhin et al suggested size-independent increases in muscle contractile function due to increases in myofibrillar packing.<sup>10</sup> Williams and Goldspink demonstrated that muscle fiber lengths increased non-linearly over the lifespan of the mouse in the soleus and biceps brachii muscles.<sup>20</sup> However, there are no data quantifying rotator cuff muscle architectural changes as a function of age in rats or any other animal. The age ranges used during these experiments is wide; 13 to 34 weeks age,<sup>1; 8; 9; 12; 19</sup> and the growth rates of the shoulder muscles are unknown during this timeframe. Since humans typically develop degenerative rotator cuff tears after skeletal maturity, rat models of muscle pathology must account for the intrinsic changes that occur in muscle architecture throughout the rat's lifespan. The purpose of this study was to examine the architecture of the rat rotator cuff muscles across different age groups, in order to uncouple the effects of aging/growth and tendon tear. We predicted that rat rotator cuff

muscles undergo age-related maturation, which results in nonlinear architectural changes over the animal's lifespan.

## METHODS

This is a cross-sectional study muscle architectural dimension across the rat lifespan. Thirty healthy Sprague-Dawley rats were euthanized under protocol approved by the Institutional Animal Care and Use Committee of the University of California, San Diego. Animals were weighed and subdivided into 6 approximate age groups based on total body mass: ~3 weeks (51-70 g, n=4), ~1 month (100-108 g, n=4), ~2 months (229-263 g, n=7), ~3 months (370-409 g, n=8), ~12 months (602-705 g, n=3), and ~18 months (760-814 g, n=4). Animals masses were chosen to gain an understanding of the entire lifespan and to best include the body mass range (400-600g) that is commonly used for rat rotator cuff experiments.<sup>9; 15; 19</sup>

Immediately following euthanasia, bilateral shoulders were skinned, and the scapulae, soft tissues, and proximal humeri were harvested en bloc. One shoulder from each animal was fixed in 10% Formalin in anatomical resting position for 48 hours while the contralateral shoulder was frozen for use in future studies.

### Skeletal Muscle Architecture

The supraspinatus and infraspinatus muscles and tendons were sharply dissected intact with their bony attachments. The epimysium was removed, and each muscle was blot-dried and weighed. Muscle length was measured as the distance from the origin of the most proximal muscle fibers to the insertion of the most distal fibers (Fig. 1), which excluded tendon proper from our measures of muscle length. Fiber length ( $L_f$ ) was measured at 4 predetermined regions (2 anterior, 2 posterior) from the supraspinatus muscle and 3 predetermined regions (1 anterior, 1 central, 1 posterior) from the infraspinatus muscle using a digital caliper (accuracy, 0.01 mm; Fig. 1).<sup>19</sup> Surface muscle fiber pennation angle relative to the axis of force generation was measured in each region with a standard goniometer as the angle between the fibers in each region and the distal muscle tendon (accuracy, 5°). Muscle fiber bundles were carefully dissected from the proximal tendon to the distal tendon of each muscle region. Fascicles were then placed in mild sulfuric acid solution (15% v/v) for 30 minutes to partially digest surrounding connective tissue, and then rinsed in phosphate buffered saline. Under magnification, 3-5 small muscle fiber bundles (consisting of approximately 20 single fibers) were isolated from each muscle region and mounted on slides. Sarcomere length ( $L_s$ ) was determined in at least 3 locations in each fiber bundle, yielding a minimum of 27 measurements of sarcomere length per muscle. Measurements were made by laser diffraction using the zero-to-first-order diffraction angle, as previously described.<sup>13,19</sup> Importantly, this technique captures the average sarcomere length in the laser-illuminated area, which contains thousands of individual sarcomeres. This sampling paradigm yields coefficients of variation on the order of 1% in a whole muscle, suggesting that sarcomere length does not vary substantially between different regions of the muscle in the anatomical position. Values for sarcomere number ( $S_n$ ) or normalized fiber length ( $L_f$ ) were then calculated for the isolated bundles according to the following equations:

$$S_n = \frac{L_f'}{L_s'}$$

and

$$L_f = L_f' \left( \frac{2.4 \mu m}{L_s'} \right)$$

where  $L_f'$  is the measured fiber length,  $L_s'$  is the measured sarcomere length in each fiber bundle,  $L_f$  is normalized muscle fiber length, and  $2.4 \mu m$  represents the optimum sarcomere length for rat muscle.<sup>17</sup> Physiological cross-sectional area (PCSA) was calculated according to the following equation:<sup>14</sup>

$$PCSA (mm^2) = \frac{M (g) \bullet \cos \theta}{\rho (g/m^3) \bullet L_f (mm)}$$

where  $M$  is muscle mass,  $\theta$  is pennation angle, and  $\rho$  is muscle density ( $1.056 \text{ g/cm}^3$ ).<sup>18</sup> Although our measurements of pennation angle are relatively coarse ( $\sim 5^\circ$ ), the effect on PCSA is less than 1%.

### Humeral Head Radius

Soft tissues were removed from the proximal humerus using sharp dissection. Superior-inferior and anterior-posterior humeral head radii were measured across the anatomical neck using a digital caliper (accuracy, 0.01 mm).

### Statistics

Linear and non-linear regression was used to assess the relationships between body mass and skeletal dimensions and muscle architecture. All statistical analyses were performed using SPSS 20.0 (IBM, Armonk, NY) with a statistical threshold of  $\alpha < 0.05$ . When regression relationships were significant, trendlines, equations, and  $r^2$  values were reported in the figure legends. Post-hoc power analyses of non-significant statistical tests yielded powers of greater than 90% in all cases.

## RESULTS

Muscle mass increased linearly with body mass in both the supraspinatus and infraspinatus muscles (Fig. 2A and 3A). However, normalized fiber bundle length increased nonlinearly (logarithmically) with total body mass (Fig. 2B and 3B). There was a weak relationship in the supraspinatus and no relationship in the infraspinatus between total body mass and sarcomere length, which remained constant at approximately  $2.4 \mu m$  (Fig. 2C and 3C) in both muscles. The development of PCSA was dominated by muscle mass and also increased linearly with total body mass (Fig. 2D and 3D).

To further explore the relationship between normalized muscle fiber bundle length and total body mass, we compared total body mass to skeletal dimensions. These data suggested that the radii of the humeral head along the superoinferior axis and the anteroposterior axis (approximately the moment arm for the supraspinatus and infraspinatus muscles, respectively) are both non-linearly (logarithmically) related to total body mass (Fig. 4A and 4D). Given that fiber length and skeletal dimensions are non-linearly (logarithmically) related to total body mass, we examined the relationship between normalized muscle fiber bundle length and humeral head radii and found that these variables were linearly related (Fig. 4B and 4C). Importantly, there was only a weak relationship between supraspinatus sarcomere length and humeral head radius and no relationship between infraspinatus sarcomere length and humeral head radius (Fig. 4C and 4F). Therefore, as the rat's skeleton (and therefore moment arms) grows, muscle fiber bundle length (serial sarcomere number) increases proportionally, which allows sarcomere length to be essentially conserved in these muscles.

## DISCUSSION

These results suggest that the architecture of the rat rotator cuff, in general, develops proportionally with total body mass. In particular, the mass of the muscle dominates the PCSA, and therefore, we would expect that force generating capacity increases linearly with body mass. Perhaps most interestingly, normalized muscle fiber bundle length increased non-linearly with total body mass, allowing sarcomere length to be conserved. When these relationships were further explored, we observed that skeletal dimensions (humeral head radius) also increased nonlinearly with total body mass. The skeleton therefore grows disproportionately fast relative to total body mass early in life, as demonstrated previously in the hindlimbs of Wistar rats.<sup>16</sup> However, fiber length tracked the growth rate of the skeleton, allowing sarcomere length to remain highly conserved. This is a critical relationship, as muscles are extremely length sensitive. This also suggests that an underlying developmental strategy exists to define sarcomere length for a particular muscle and to retain that sarcomere length over the lifespan of the animal. This developmental strategy has been speculated in muscles of the rat hindlimb<sup>16</sup>, but only demonstrated in two muscles of the mouse.<sup>20</sup> Furthermore, because skeletal dimensions (humeral head radius) scale linearly with fiber bundle length, we would expect that the range of sarcomere lengths achieved over a given range of joint positions (sarcomere length operating range) would also be conserved.

To our knowledge, the observation of conserved sarcomere length and sarcomere length operating range in rotator cuff muscles has never been quantified. There are a number of basic science and clinical implications for this important observation. First, the rules and regulatory factors involved in the development of muscle architecture are still largely unknown. These results suggest that preservation of sarcomere length may be one such “rule”. These rules may be dictated by a number of autocrine, paracrine, and/or endocrine factors. Of particular recent interest is the role of bone in regulating muscle growth and development. Specifically, bone has recently been described as a potential “endocrine hub” regulating whole-organism physiology, and the existence of bone-derived hormones regulating skeletal muscle growth and adaptation is an interesting potential mechanism.<sup>11</sup> Secondly, based on the non-linear increase in fiber length early in life, these results suggest

that the ability to regulate sarcomere number may change over the lifespan. This idea would need to be explored experimentally, but it has profound implications for muscle recovery over the lifespan. Clinically, regulation of sarcomere number is important in all forms of tenotomy (including rotator cuff tears) because alterations in muscle fiber length directly affect muscle performance.<sup>19</sup> Our results indicate that there is an overall developmental strategy to regulate sarcomere length (and number), so changes in fiber length as a result of experimentally induced tendon failure should consider the normal growth trajectory of the muscle when examining differences between injured and uninjured tendons.

There are a number of important limitations to this study. At this stage, these results are applicable to two rat rotator cuff muscles in a body mass range of 51-814 grams. Extrapolating these developmental strategies (and certainly the developmental rates) to different animal models or different masses is, perhaps, premature. However, the use of regression-based statistics and the wide range of animals masses used in this study has yielded adequate power to our statistical analyses, making us confident in our results. Second, we have theorized that skeletal dimensions direct the development of muscle architecture, but this is merely an observed correlation. We have not experimentally arrested growth of the skeleton to see if muscle architecture is similarly arrested, nor have we experimentally manipulated muscle architecture to see if skeletal architecture is changed. It is possible that there is some two-way communication between the muscle and the skeleton, even if it is just mechanical in nature.

## CONCLUSIONS

In conclusion, the development of muscle architectural features in the rat rotator cuff muscles follows linear and non-linear growth trajectories. Using these data in the body mass range of 400 – 600 grams, as frequently seen in experimental models of rotator cuff tendon injury, a 30% increase in supraspinatus and infraspinatus muscle mass was observed. Similarly, a 7% increase in fiber length, a 27% increase in PCSA, and nearly constant sarcomere lengths were observed. These data indicate that investigators should expect significant changes in muscle architecture during the course of an experimental tear and/or repair period in this animal model. Over the lifespan, the development of force production appears to follow a linear trajectory with total body mass, but development of muscle fiber length appears to be non-linear and designed to conserve sarcomere length.

## Acknowledgments

Funding Support: The sources of funding for this study were; NIH R01 AR057836, NIH R24 HD050837, and NIH P30 AR057235

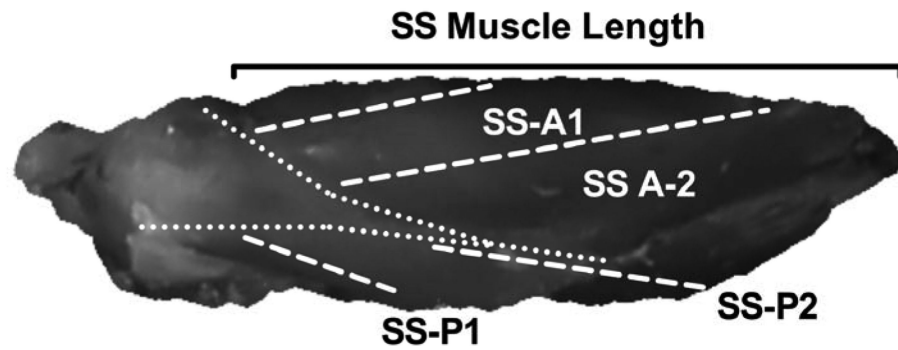
## References

1. Barton ER, Gimbel JA, Williams GR, Soslowsky LJ. Rat supraspinatus muscle atrophy after tendon detachment. *J Orthop Res.* 2005; 23:259–65. doi: 10.1016/j.orthres.2004.08.018. [PubMed: 15734235]
2. Bodine SC, Roy RR, Meadows DA, Zernicke RF, Sacks RD, Fournier M, et al. Architectural, histochemical, and contractile characteristics of a unique biarticular muscle: the cat semitendinosus. *J Neurophysiol.* 1982; 48:192–201. [PubMed: 7119845]

3. Davidson PA, Rivenburgh DW. Rotator cuff repair tension as a determinant of functional outcome. *J Shoulder Elbow Surg.* 2000; 9:502–6. [PubMed: 11155303]
4. Fuchs S, Chylarecki C, Langenbrinck A. Incidence and symptoms of clinically manifest rotator cuff lesions. *Int J Sports Med.* 1999; 20:201. [PubMed: 10333099]
5. Gans C. Fiber architecture and muscle function. *Exerc Sport Sci Rev.* 1982; 10:160–207. [PubMed: 6749514]
6. Gerber C, Meyer DC, Schneeberger AG, Hoppeler H, von Rechenberg B. Effect of tendon release and delayed repair on the structure of the muscles of the rotator cuff: an experimental study in sheep. *J Bone Joint Surg Am.* 2004; 86-A:1973–82. No doi. [PubMed: 15342760]
7. Gerber C, Schneeberger AG, Hoppeler H, Meyer DC. Correlation of atrophy and fatty infiltration on strength and integrity of rotator cuff repairs: a study in thirteen patients. *J Shoulder Elbow Surg.* 2007; 16:691–6. doi:10.1016/j.jse.2007.02.122. [PubMed: 17931904]
8. Gimbel JA, Mehta S, Van Kleunen JP, Williams GR, Soslowky LJ. The tension required at repair to reappose the supraspinatus tendon to bone rapidly increases after injury. *Clin Orthop.* 2004; 426:258–65. doi: 10.1097/01.blo.0000136831.17696.80. [PubMed: 15346083]
9. Gimbel JA, Van Kleunen JP, Mehta S, Perry SM, Williams GR, Soslowky LJ. Supraspinatus tendon organizational and mechanical properties in a chronic rotator cuff tear animal model. *J Biomech.* 2004; 37:739–49. doi: 10.1016/j.jbiomech.2003.09.019. [PubMed: 15047003]
10. Gokhin DS, Ward SR, Bremner SN, Lieber RL. Quantitative analysis of neonatal skeletal muscle functional improvement in the mouse. *J Exp Biol.* 2008; 211:837–43. doi:10.1242/jeb.014340. [PubMed: 18310108]
11. Karsenty G, Ferron M. The contribution of bone to whole-organism physiology. *Nature.* 2012; 481:314–20. doi:10.1038/nature10763. [PubMed: 22258610]
12. Kim HM, Galatz LM, Lim C, Havlioglu N, Thomopoulos S. The effect of tear size and nerve injury on rotator cuff muscle fatty degeneration in a rodent animal model. *J Shoulder Elbow Surg.* 2012; 21:847–58. doi:10.1016/j.jse.2011.05.004. [PubMed: 21831663]
13. Lieber RL, Yeh Y, Baskin RJ. Sarcomere length determination using laser diffraction. Effect of beam and fiber diameter. *Biophys J.* 1984; 45:1007–16. [PubMed: 6610443]
14. Powell PL, Roy RR, Kanim P, Bello M, Edgerton VR. Predictability of skeletal muscle tension from architectural determinations in guinea pig hindlimbs. *J Appl Physiol.* 1984; 57:1715–21. [PubMed: 6511546]
15. Soslowky LJ, Carpenter JE, DeBano CM, Banerji I, Moalli MR. Development and use of an animal model for investigations on rotator cuff disease. *J Shoulder Elbow Surg.* 1996; 5:383–92. [PubMed: 8933461]
16. Tamaki T, Uchiyama S. Absolute and relative growth of rat skeletal muscle. *Physiol Behav.* 1995; 57:913–9. [PubMed: 7610144]
17. ter Keurs HE, Luff AR, Luff SE. Force--sarcomere-length relation and filament length in rat extensor digitorum muscle. *Adv Exp Med Biol.* 1984; 170:511–25. [PubMed: 6540041]
18. Ward SR, Lieber RL. Density and hydration of fresh and fixed human skeletal muscle. *J Biomech.* 2005; 38:2317–20. doi:10.1016/j.jbiomech.2004.10.001. [PubMed: 16154420]
19. Ward, SR.; Sarver, JJ.; Eng, CM.; Kwan, A.; Wurgler-Hauri, CC.; Perry, SM., et al. *J Orthop Sports Phys Ther.* Vol. 40. 2477: 2010. Plasticity of muscle architecture after supraspinatus tears.; p. 729-35.doi:10.2519/jospt.2010.3279
20. Williams PE, Goldspink G. Longitudinal growth of striated muscle fibres. *J Cell Sci.* 1971; 9:751–67. [PubMed: 5148015]
21. Winters TM, Takahashi M, Lieber RL, Ward SR. Whole muscle length-tension relationships are accurately modeled as scaled sarcomeres in rabbit hindlimb muscles. *J Biomech.* 2011; 44:109–15. doi:10.1016/j.jbiomech.2010.08.033. [PubMed: 20889156]



A



B

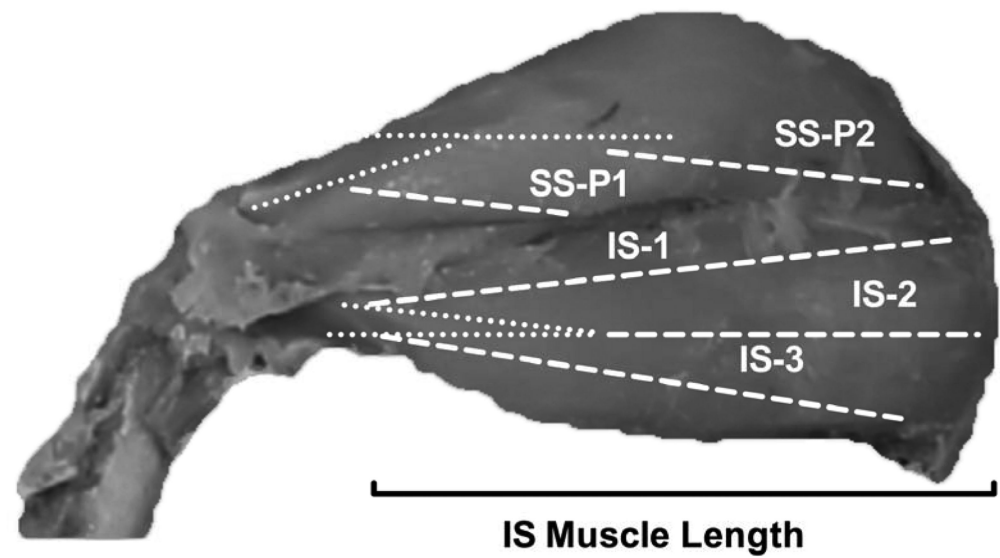


**Figure 1.**

Representative superior (A) and posterior (B) images of the rotator cuff. Dashed white lines represent the different sampling regions of the supraspinatus (SS) and infraspinatus (IS). Dotted white lines mark the borders of the deep tendons. Solid black brackets denote the muscle length for the supraspinatus (A) and infraspinatus (B). A=Anterior; P=Posterior.



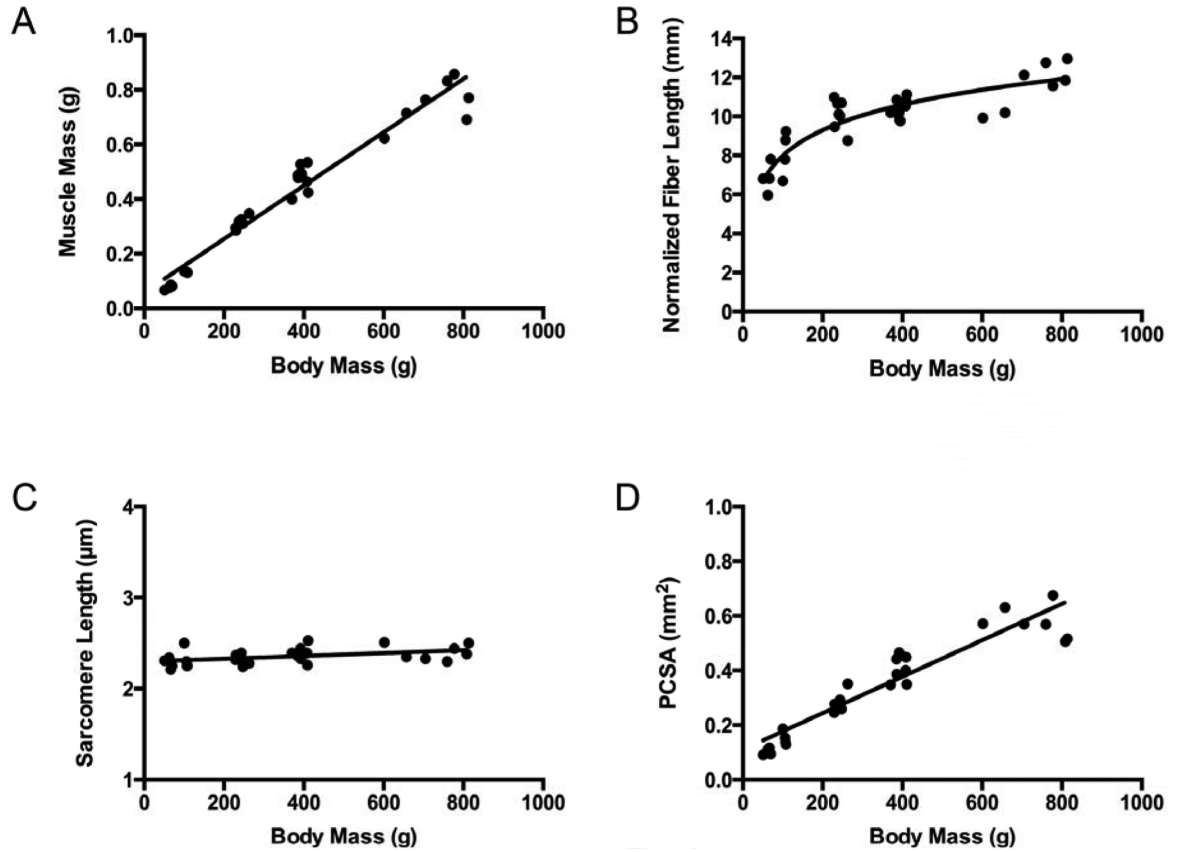


**Figure 2.**

Supraspinatus muscle architectural features increase as a function of animal mass (age), except for sarcomere length, which remains constant over the lifespan. Muscle mass (A) ( $y = 0.001x + 0.0588$ ,  $r^2 = 0.957$ ,  $p < 0.0001$ ) increases linearly, normalized muscle fiber bundle length (B) ( $y = 1.888\ln(x) - 0.7084$ ,  $r^2 = 0.797$ ) increases non-linearly, sarcomere length (C) ( $y = 0.000156x + 2.298$ ,  $r^2 = 0.20$ ,  $p = 0.012$ ) increases linearly, and physiological cross-sectional area (PCSA) (D) ( $y = 0.0007x + 0.1105$ ,  $r^2 = 0.876$ ,  $p < 0.0001$ ) increases linearly as a function of total body mass.

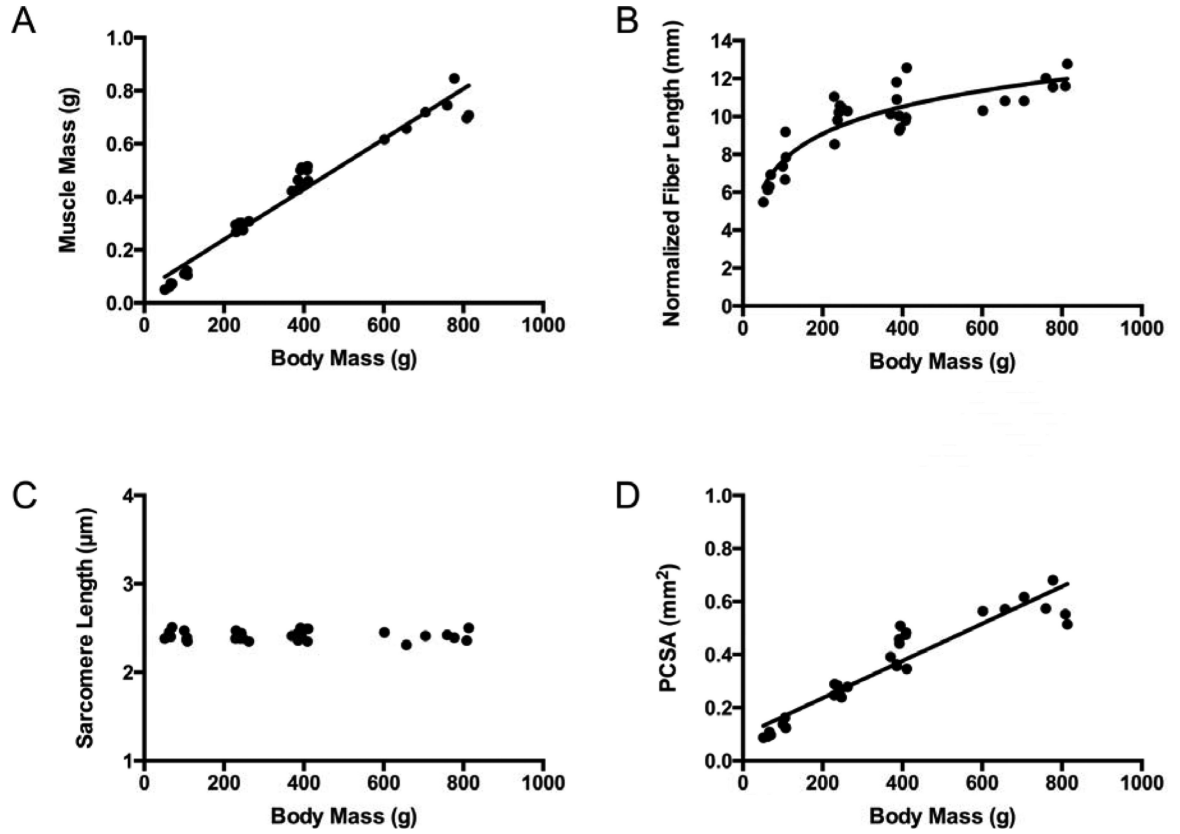


**Figure 3.**

Infraspinatus muscle architectural features increase as a function of animal mass (age), except for sarcomere length, which remains constant over the lifespan. Muscle mass (A) ( $y = 0.0009x + 0.0493$ ,  $r^2 = 0.954$ ,  $p < 0.0001$ ) increases linearly, normalized muscle fiber bundle length (B) ( $y = 2.0693\ln(x) - 1.8853$ ,  $r^2 = 0.783$ ) increases non-linearly, sarcomere length (C) does not change ( $r^2 = 0.000252$ ,  $p = 0.932$ ), and physiological cross-sectional area (PCSA) (D) ( $y = 0.0007x + 0.0957$ ,  $r^2 = 0.884$ ,  $p < 0.0001$ ) increases linearly as a function of total body mass.

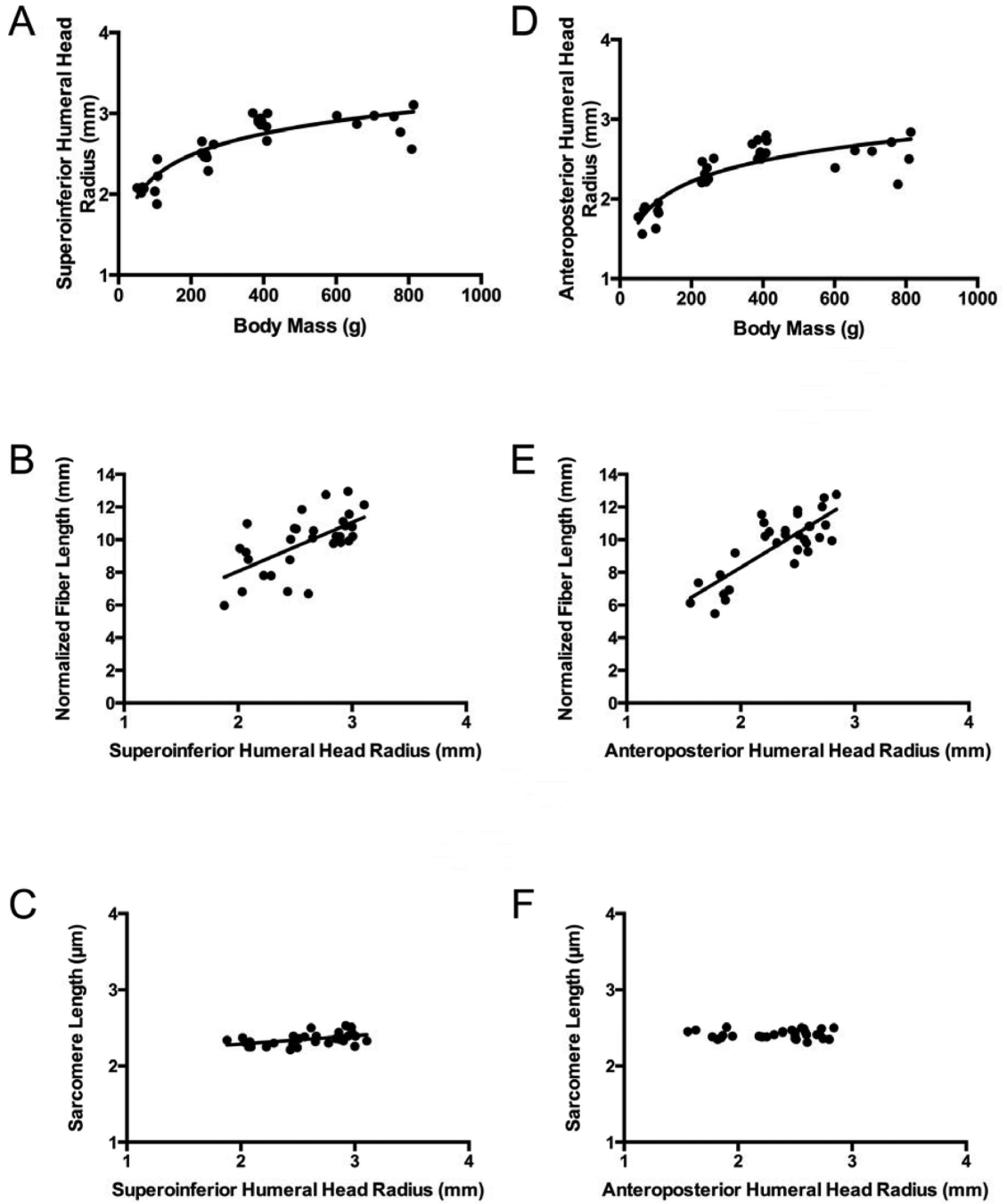


**Figure 4.** The superoinferior humeral head radius increases non-linearly as a function of body mass (A) ( $y = 0.3839\ln(x) + 0.4537$ ,  $r^2 = 0.770$ ), which allows normalized muscle fiber bundle length to increase linearly with superoinferior humeral head radius (B) ( $y = 1.8779x + 0.0981$ ,  $r^2 = 0.601$ ,  $p = 0.0002$ ), allowing sarcomere length to remain constant versus superoinferior humeral head radius (C) in the supraspinatus muscle ( $y = .114x + 2.057$ ,  $r^2 = 0.242$ ,  $p = 0.005$ ). Similarly, the anteroposterior humeral head radius increases non-linearly with total body mass (D) ( $y = 0.3798\ln(x) + 0.2043$ ,  $r^2 = 0.735$ ), which allows normalized

muscle fiber bundle length to increase linearly with anteroposterior humeral head diameter (E) ( $y = 2.1182x - 0.1766$ ,  $r^2 = 0.644$ ), allowing sarcomere length to remain constant versus anteroposterior humeral head radius ( $r^2 = 0.002$ ,  $p = 0.8179$ ) (F) in the infraspinatus muscles.